

Fracture Behavior of Aged 15Cr-5Ni Stainless Steel

15Cr-5Ni 스테인리스강의 파괴 거동

M. C. Chu, K. Saito, M. Tubota and K. Ando

Key Words : Precipitation hardening stainless steels(석출 강화 스테인리스강), Fatigue crack growth(피로 크랙 성장), Fatigue crack initiation(피로 크랙 발생), Fatigue strength(피로 강도), Fracture toughness(파괴 인성), Notch radius(노치 반경)

Abstract : 15Cr 5Ni 석출강화 스테인리스강 3종류의 피로균열 발생과 성장 특성 및 파괴인성에 대하여 노치함수로서 연구하였다. 3종류강의 열처리 조건은 482 °C, 579 °C 및 621 °C이다. 621 °C에서 4시간동안 열처리한 시험편 C는 약 280 MPa √m의 가장 높은 파괴인성을 보였으며, 3종류에서 피로균열 성장이 가장 늦었다. 482 °C에서 1시간 열처리한 시험편 A에서, 피로균열발생한계, ΔK_{th}, 는 노치반경0.3 mm에서 약 20 MPa √m의 가장 높은 값을 보였다. 시험편 A는 시험편 B와 C보다 피로균열 성장이 빨랐지만, 피로균열 발생이 늦었다. 예 하중에 의한 노치선단의 압축잔류응력은 노치 시험편의 피로강도 향상에 유용한 방법이었다.

1. INTRODUCTION

Precipitation Hardening (PH) martensitic stainless steels have stress corrosion resistance with high tensile strength. Thus, some researchers have been studying actively the effect of precipitation hardening on stainless steel[1,2]. Especially, 15 5 precipitation hardening (PH) stainless steel, which contains both about 15 % Cr and 5 % Ni, is a high strength material that was prepared by precipitating Cu elements. Because of its high quality, the material has been used in structural elements, which requires a high reliability, such as the space shuttle and nuclear power plants. Therefore, it is very important to clarify the mechanical properties such as fracture toughness and fatigue behaviour.

In this study, from this point of view, the

fracture toughness and the resistance to fatigue crack growth and initiation of 15 5 PH stainless steels which were heat treated at various temperatures were investigated. The effect of pre loading on fatigue crack initiation life of notched specimen is also discussed.

2. EXPERIMENTAL PROCEDURE

2.1 Materials and Specimen

The chemical composition of 15 5PH (Precipitation Hardening) stainless steel is listed in Table 1. This material contained about 15 mass% of Cr and 5 mass% of Ni, respectively. Especially, about 3 mass% of Cu was contained in this material as a precipitate. The material was solution treated at 1038 °C for 1 hour and then heat treated at temperature of 482 °C, 579 °C and 621 °C, respectively, see Table 2. The mechanical properties of tested materials are also listed in Table 2. Specimen A has the highest tensile strength of 1365 MPa and Vickers hardness of 440, and specimen C has the lowest tensile strength 1073 MPa and Vickers

접수일 : 2001년 12월 5일

M. C. Chu, K. Ando : Department of Energy & Safety Engineering, Yokohama National University

K. Saito : Department of Energy & safety Engineering Yokohama National University

M. Tubota : Heavy Apparatus Engineering Laboratory Toshiba Corporation

Table 1 Chemical composition of the material [mass%].

C	Si	Mn	P	S	Ni	Cr	Mo	Cu	Nb	Ta
0.03	0.61	0.69	0.009	0.003	4.19	15.09	0.01	3.26	0.27	<0.01

Table 2 Heat treatment Conditions.

Sample Name	Solution Heat Treatment	Precipitation Hardening Heat treatment	Tensile Strength(MPa)	Yielding Strength(MPa)	Vickers Hardness
Specimen A	1038°C × 1h	482°C × 1h	1365	1262	440
Specimen B		579°C × 1h	1073	1040	360
Specimen C		621°C × 1h	941	775	319

hardness of 319. Specimen B, on the other hand, has the middle ones.

2.2 Experimental Method

The dimension and shape of the specimens are shown in Fig. 1. The specimen type A, see Fig. 1 (a), was used for fracture toughness test and fatigue crack growth test while the specimen type B, see Fig. 1 (b), was applied for fatigue crack initiation test.

The fracture toughness test was carried out at room temperature in accordance with ASTM E339 83 [3] and ASTM E813 89 [4]. The fatigue crack growth tests were conducted at room temperature using an electrohydraulic fatigue test machine in accordance with ASTM E647 95a [5]. The test conditions were as follow: sine wave loading, frequency of 3 10 Hz and stress ratio, R 0.1.

The fatigue crack initiation tests were performed using notched CT specimen with a notch radius of 0.1 and 0.3 mm. These tests were performed at a frequency of 10 30 Hz, R 0.1, sine wave at room temperature in air.

To investigate the effect of compressive residual stresses on the fatigue strength of notched specimen, notched specimens were tensile preloaded.

The pre load were applied of 8kN and 12kN and the test was carried out at room temperature in air.

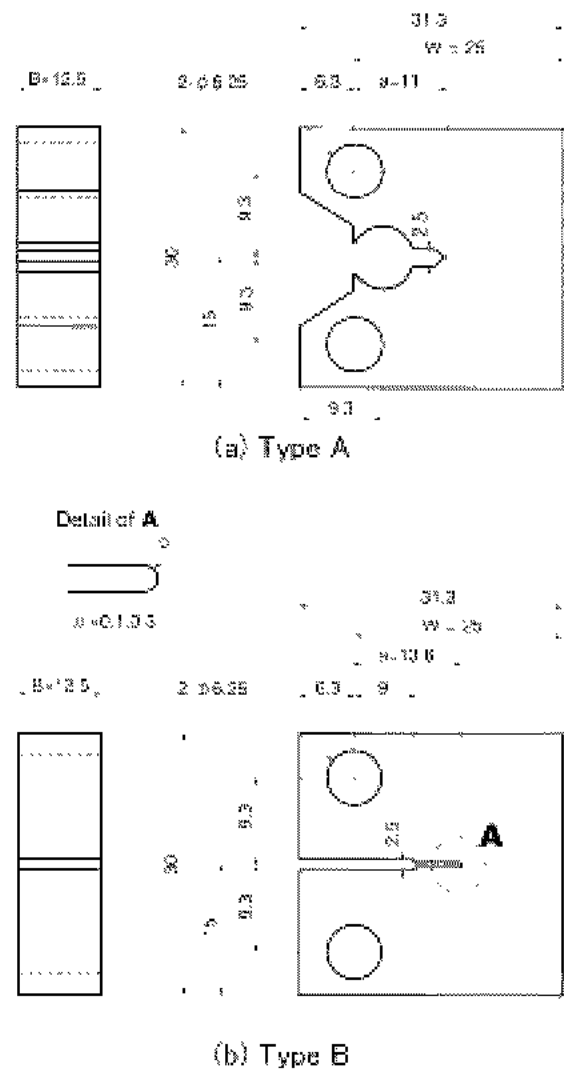


Fig. 1 Dimension and shape of specimens

3. RESULTS AND DISCUSSION

3.1 Fracture Toughness

Typical load displacement curves of specimen A, B and C are shown in Fig. 2. In specimen A, see Fig. 2, fracture toughness was evaluated in accordance with ASTM E339 83 because a linear relationship was observed between load and displacement. On the other hand, in case of specimen B and C, fracture toughness was evaluated in accordance with ASTM E339 89 because of its non linear relationship. Especially, a fracture pattern of specimen C showed a remarkable ductility and stable crack growth was observed. Thus, fracture toughness value

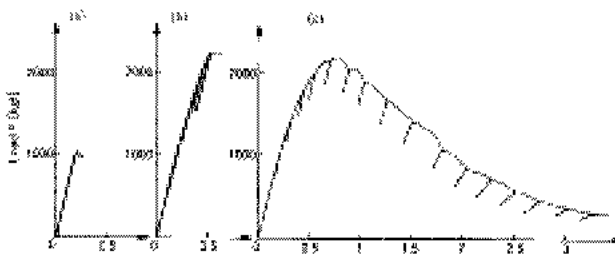


Fig. 2 Displacement at load point, [mm]

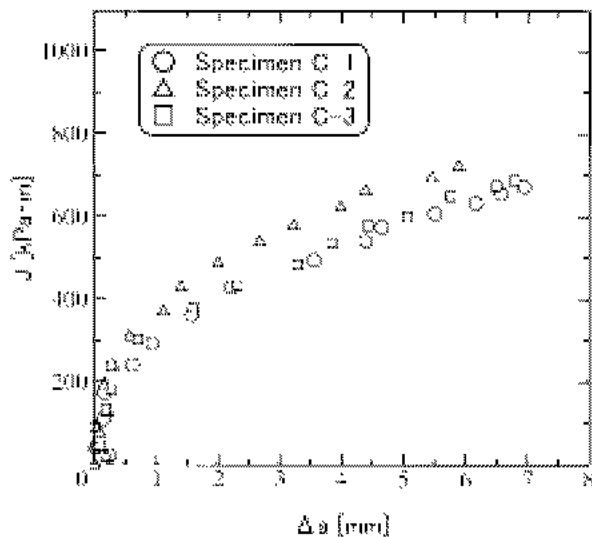
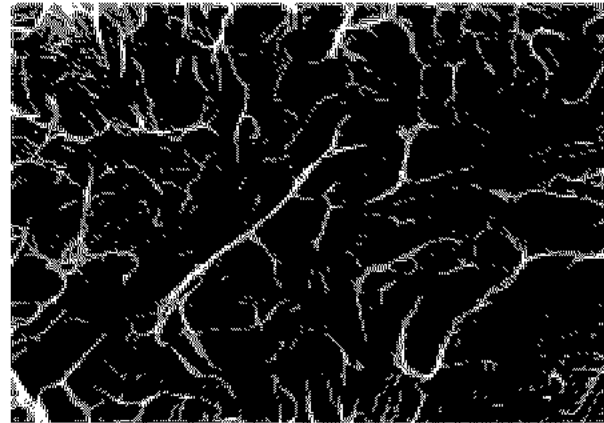
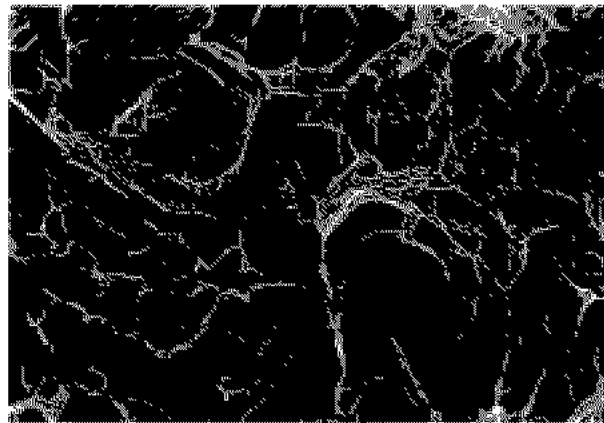


Fig. 3 J R curves of specimen C

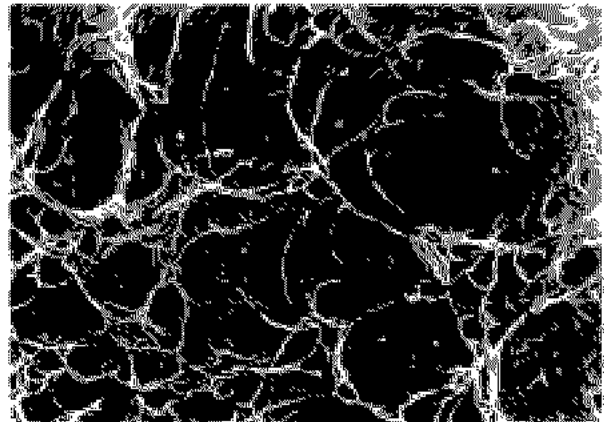
was determined using J R curve. The results are shown in Fig. 3. Three test specimens were used in this experiment. Resistance to stable crack growth, dJ/da , was about 62, 62 and 60 $kPa \cdot m/mm$ for test specimen of C1, C2 and



(a) Specimen A



(b) Specimen B



(c) Specimen C

30 30

Fig. 4 SEM photographs of fracture surface of (a) Specimen A, (b) specimen B and (c) Specimen C.

C3, respectively. The test results of fracture toughness are listed in TABLE 3. Specimen C which was heat treated at 621 °C for 4 hour,

Table 3 Fracture toughness test results.

Sample Name	Fracture toughness [MPa · m ^{0.5}]			Remark
Specimen A	54.7	53.2		K _{IC}
Specimen B	166.6	172.2	149.8	K _C (J)
Specimen C	255.6	297.1	287.2	K _{IC} (J)

the average fracture toughness value, K_{IC}(J), is about 280 MPa√m, and is higher than that of specimen A or B.

Fig. 4 shows the SEM photographs of fracture surface for specimen A, B and C. In specimen A, see Fig. 4(a), the cleavage fracture planes were observed mainly on all fracture surfaces. It is considered that fracture toughness of specimen A shows the lowest value of about 50 MPa√m due to its cleavage fracture. In specimen C that has the highest toughness value, small and large dimples were observed on the fracture surface. On the other hand, fracture surface of specimen B were consisted of both small dimples(<5μm) and cleavage fracture planes.

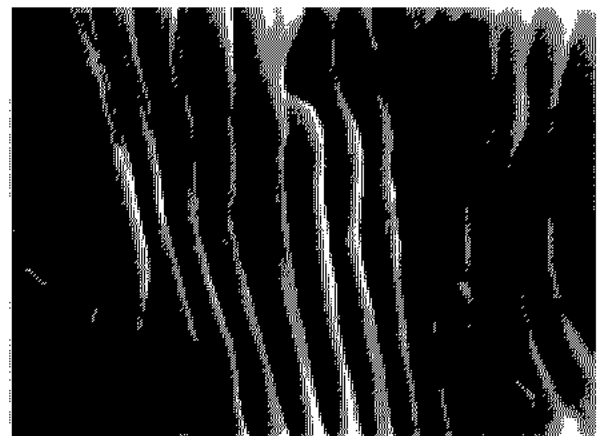
3.2 Fatigue Crack Growth Behaviour

Fig. 5 shows relationship between crack growth rate, da/dN, and stress intensity factor range, ΔK, of specimens A, B and C. The m value of specimen A, B and C is 4.02, 3.17 and

3.02 respectively. From this figure, it is can be seen that specimen A had the lowest resistance to fatigue crack growth compared to specimens B and C. In contrast, specimen C that was heat treated at higher temperature of 621 °C than that of specimen A and B, showed the lowest fatigue crack growth rate, i.e., specimen C has the highest resistance to fatigue crack growth. However, the threshold stress intensity factor, Δ



(a) Intergranular fracture 20 μm



(b) Fracture 1 μm

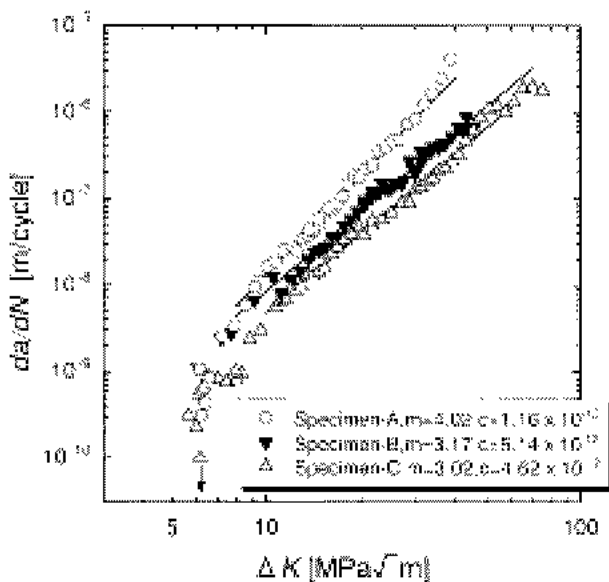


Fig. 5 Relationship between crack growth rate and stress intensity factor range

Fig. 6 SEM photographs of fatigue fracture surface of specimen B

K_{th} , is about $6 \text{ MPa}\sqrt{\text{m}}$ and showed the same value for all materials.

SEM photographs of fracture surface for specimen B are shown in Fig. 6. The intergranular fracture planes were mainly observed on fatigue fracture surface when the specimen applied at stress of ΔK of $< 15 \text{ MPa}\sqrt{\text{m}}$, which was shown in Fig. 6(a). Besides, on the fatigue fracture surface where applied at high ΔK of $> 40 \text{ MPa}\sqrt{\text{m}}$, the striation could be observed frequently. The SEM photograph of striation, see Fig. 6(b), where had been formed at $\Delta K = 40 \text{ MPa}\sqrt{\text{m}}$, the distance of striation is about $0.5 \mu\text{m}$ and it was in agreement with the results of Fig. 5. However, the intergranular fracture plane and the striation could not be observed on the fatigue fracture surface of specimen A.

3.3 Fatigue Crack Initiation Life of the Notched Specimen

Fig. 7 shows that the relationship between the number of cycles to fatigue crack initiation life, N_i , and stress intensity factor range, ΔK_p , as a function of notch radius, ρ . N_i is a number of cycles when fatigue crack was initiated and then propagated over a distance of 0.5 mm from the notch tip. For all specimens, ΔK_p decrease with increasing fatigue crack initiation life.

The fatigue crack initiation limit, $\Delta K_{p,lim}$, was defined as the ΔK_p at which the fatigue crack had not initiated on specimen surface until the number of cycles reached to 2×10^6 cycles. The $\Delta K_{p,lim}$ at $\rho = 0.3 \text{ mm}$ is higher than that of at $\rho = 0.1 \text{ mm}$ for all specimen, see Fig. 7(a), (b) and (c). When notch radius, ρ , is 0.1 mm , see Fig. 7(d), the $\Delta K_{p,lim}$ of specimen C is about $10 \text{ MPa}\sqrt{\text{m}}$ and is higher than that of specimen B and C. In case of $\rho = 0.3 \text{ mm}$, however, fatigue crack initiation, $\Delta K_{p,lim}$, of specimen A was about $20 \text{ MPa}\sqrt{\text{m}}$ which was the highest value of among the specimen A, B and C. From the above results, it is concluded that specimens C heat treated at $621 \text{ }^\circ\text{C}$ have a low resistance to fatigue crack initiation when ρ is 0.3 mm although it have a high toughness.

In contrast, specimen A has no good

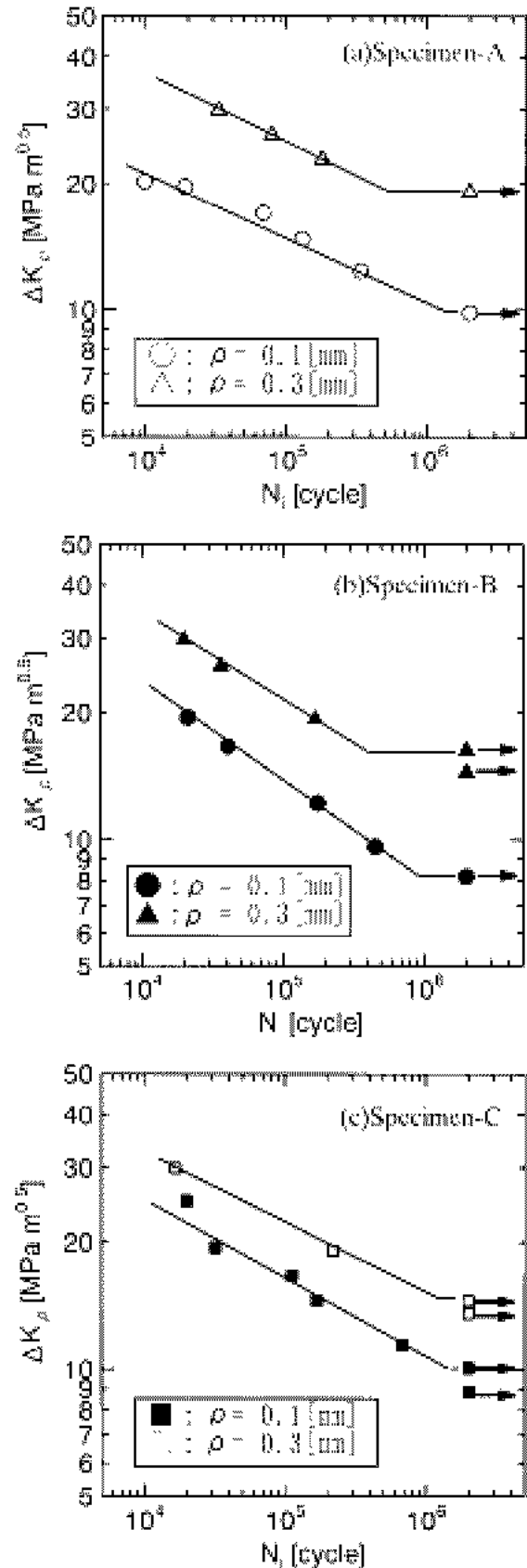


Fig. 7 Relationship between the number of cycles to fatigue crack initiation life, N_i , and stress intensity factor range, ΔK_p , as a function of notch radius.

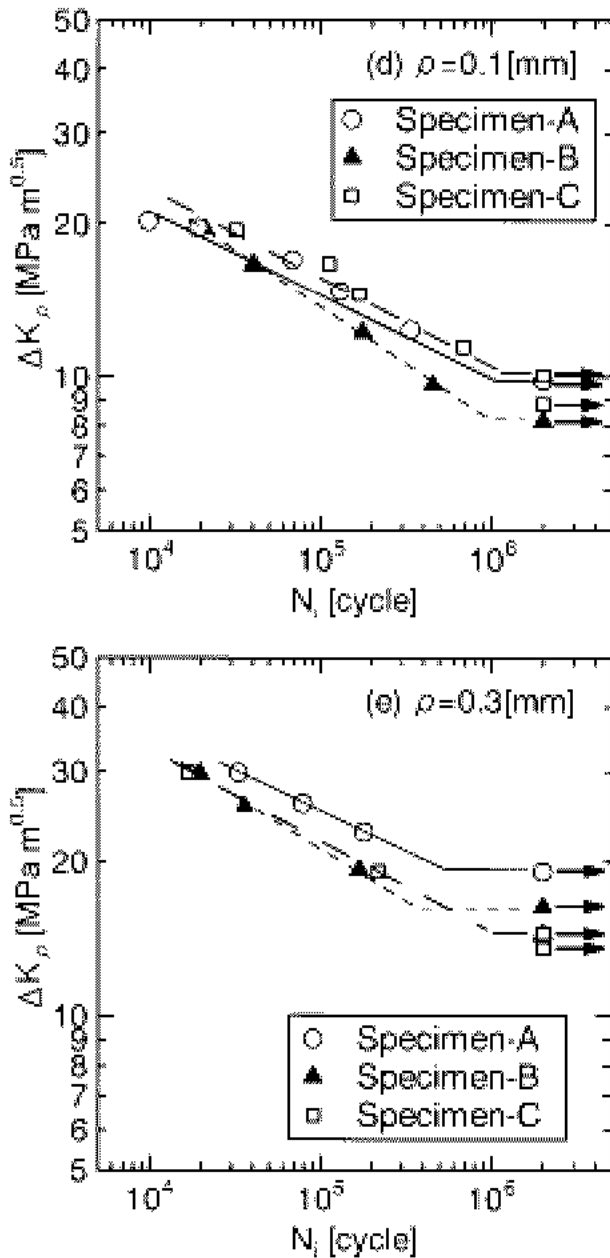


Fig. 7 Continued (d), (e)

resistance to fatigue crack growth but has a high resistance to fatigue crack initiation in comparison with specimen C when ρ is 0.3 mm. It may be considered that the improved resistance to fatigue crack initiation caused to its high hardness and tensile strength. But, at ρ 0.1 mm, the resistance to crack initiation of specimen A shows a little lower than that of specimen C. On the other hand, a lowering rates of fatigue crack initiation limit is denoted α , $\alpha = 1 - (\Delta K_{p, 0.1mm, lim} / \Delta K_{p, 0.3mm, lim}) \times 100\%$. The α of specimen C is about 32% and showed the lowest value among the

specimen A, B and C. This means that the resistance to fatigue crack initiation of specimen C is less sensitive to the stress concentration in comparison with specimen A and B.

3.4 Improvement of Fatigue Strength of Notched Specimen by Pre-Loading

To improve of fatigue crack initiation resistance of notched specimen, a tensile preload was applied to the specimen before fatigue crack initiation test. In this test, the specimen C with notch radius of 0.3 mm was used. The relationship between conditions of pre loading and the fatigue crack initiation limit, $\Delta K_{p, lim}$, of the notched specimen C is shown in Fig. 8. The $\Delta K_{p, lim}$ of as received specimen is about 16 MPa \sqrt{m} . When the tensile pre load is 8kN, the $\Delta K_{p, lim}$ is about 25 MPa \sqrt{m} and improved of 93% in comparison with as received specimen. Furthermore, the $\Delta K_{p, lim}$ at a pre load of 12kN is about 30 MPa \sqrt{m} and was about two times higher than that of as received specimen. We considered that the improvement is due to the introduction of compressive residual stresses at notch tip due to pre tensile loading over yield point.

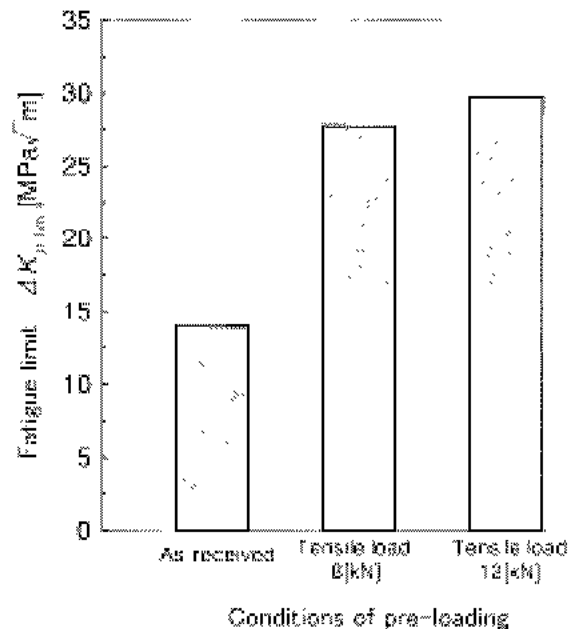


Fig. 8 Relationship between conditions of pre loading and the limit of stress intensity factor range, $\Delta K_{p, lim}$, for notched specimen.

4. CONCLUSIONS

The main test results obtained in this study are as follow:

- 1) Specimen C that was heat treated at 621°C for 4 hours has a high toughness value of about 280 MPa \sqrt{m} .
- 2) From SEM observation results, It was found that the fracture surface of specimen C was covered mainly by dimples, while the cleavage fracture planes were observed on fracture surface of specimen A. On the other hand, in specimen B, the fracture surface consisted of both small dimples and cleavage fracture planes.
- 3) Specimen A heat treated at the lowest temperature of 482 °C showed the lowest resistance to fatigue crack growth and the m value of Paris law close to 4.
- 4) For all specimens, ρ is decreased with decreasing the fatigue crack initiation limit, ΔK_{ρ} , \lim , and specimen C showed the highest resistance to fatigue crack initiation when ρ is 0.1 mm, but showed the lowest resistance at ρ 0.3 mm.
- 5) In case of ρ 0.3 mm, the fatigue crack initiation limit, ΔK_{ρ} , \lim , of specimen A showed the highest value of about 20 MPa \sqrt{m} and it can be seen that specimen A had a good resistance to fatigue crack initiation, although it had a lower resistance to fatigue crack growth than that of specimen B and C.
- 6) Introduction of compressive residual stress at notch tip due to pre loading over yield point was useful method to improve the fatigue strength of the notched specimen

AIME. 245, pp. 2135 2140, 1969

3. E399 83, Standard Test Method for K_{IC}, A Measure of Fracture Toughness. American Society for Testing & Materials. pp. 488 512, 1983
4. E813 89, Standard Test Method for J_{IC}, A Measure of Fracture Toughness. American Society for Testing & Materials. pp. 700 714, 1989
5. E647 95a, Standard Test Method for Measurement of Fatigue Crack Growth rates. American Society for Testing and Materials. pp. 565 601, 1995

REFERENCES

1. Y. Asayama, Precipitation Processes and Notched Tensile Strengths of Precipitation hardening stainless Steels. J. Japan. Inst. Metals. 45(7), pp. 731 739, 1981
2. W. C. Clarke, Jr. A Study of Embrittlement of a Precipitation Hardening Stainless Steel and Some Related materials. Trans. Met. Soc.